Original Article

Role of spectral domain optical coherence tomography in the diagnosis and prognosis of papilledema

Rakesh Panyala, Pradeep Sharma[1,2], Ramanjit Sihota[3], Rohit Saxena[3], Kameshwar Prasad[3], Swati Phuljhele[3], Sneha Gurrala[4], Karthika Bhaskaran[3]

Purpose: The study of papilledema with a novel noninvasive technique such as spectral domain-optical coherence tomography (SD-OCT) provides minute and detailed cross-sectional changes thus giving an insight into the application of biomechanical principles and pathophysiology of disc edema. **Methods:** We measured average retinal nerve fiber layer (RNFL) thickness and the retinal pigment epithelium/Bruch's membrane (RPE/BM) angle at the temporal and nasal borders of the neural canal opening (NCO) in 30 eyes with papilledema, 30 eyes with papillitis, and 80 control eyes. The inward angulation was considered as positive and the outward as negative. Follow-up was done at 1, 2, 3, and 6 months. The main outcome measures are the average RNFL thickness and the RPE/BM angle. **Results:** 29 eyes (96.6%) with papilledema had a positive RPE/BM angle (+8.11 ± 3.13). 29 eyes (96.6%) with papillitis had a negative RPE/BM angle (−1.04 ± 3.27). On follow-up at 1 month, both RNFL thickness (P = 0.01) and RPE-BM angle (P = 0.001) reduced significantly in eyes with papilledema; in eyes with papillitis, there was a significant reduction in the RNFL thickness (P = 0.02), but not in the RPE-BM angle (P > 0.05). RNFL thickness in papilledema cases normalized at 3 months whereas RPE/BM normalized at 6 months of follow-up. To detect papilledema, OCT has a sensitivity of 96.66% and specificity of 99.09% on both nasal and temporal sides. **Conclusion:** After appropriate treatment, the RPE/BM angle in papilledema decreased much later than the RNFL thickness. Hence, the RPE/BM angle in papilledema (positive) can be used to differentiate it from papillitis (negative) and also to monitor the activity of the disease.

Access this article online

Website: www.ijo.in

DOI: 10.4103/ijo.IJO_3269_20

Quick Response Code:

Key words: Idiopathic intracranial hypertension, papilledema, papillitis, RNFL thickness, RPE/BM angle, spectral domain OCT

Papilledema is caused by increased intracranial pressure (ICP). Study of the changes in optic nerve head with novel noninvasive techniques provides minute and detailed cross-sectional changes occurring in such patients, and an insight into the application of biomechanical principles and pathophysiology of disc edema.[1] Kupersmith *et al*.[2] showed how increased ICP affects the peripapillary subsurface structures of the neural canal opening (NCO) of the ONH at the level of the retinal pigment epithelium/basement membrane (RPE) and Bruch's membrane (RPE/BM) layer using spectral domain-optical coherence tomography (SD-OCT). Our study evaluates the role of these findings to monitor the treatment of papilledema in the Indian population.

Methods

This was a prospective, observational study conducted on patients with disc edema recruited from the neuro-ophthalmology clinic from December 2017 to June 2019. Ethical clearance was obtained from the Institutional Ethics Committee. Patients between 10 and 70 years of age with papilledema and papillitis were included in the study after taking consent from the patient/guardian. Healthy volunteers between 10 and 70 years of age with no signs of papilledema, other causes of disc edema, neurological disorders, or any other systemic illness were included as controls.

All subjects underwent detailed ophthalmological examination including visual acuity testing, slit-lamp examination, dilated fundus examination, color fundus photography, SD-OCT, visual fields, and intraocular pressure at baseline. Patients suspected of having a neurologic disorder underwent detailed neurologic examination, brain CT/MRI imaging, and cerebrospinal fluid analysis if required.

Using a Cirrus SD-OCT (Carl Zeiss Meditec), scans were performed in all the patients and controls at baseline and at subsequent follow-ups, and well-focused, uniformly illuminated images were obtained. The laser scanned a 6 × 6 mm area, capturing the data of optic disc cube 200 × 200 (×2) consisting of 200 A-scans from 200 linear B-scans of 2 mm

Consultant Pediatric Ophthalmology and Strabismus, MaxiVision Eye Hospital, Karimnagar, [1]Professor Head Strabismus, Pediatric Ophthalmology and Neuro-Ophthalmology, AIIMS, New Delhi, [2]Director Strabismus Pediatric and Neuro-Ophthalmology Centre for Sight, New Delhi, [3]Department of Ophthalmology, All India Institute of Medical Sciences, New Delhi, [4]MBBS, Kamineni Institute of Medical Sciences, Narketpally, Hyderabad, Telangana, India

Correspondence to: Prof. Pradeep Sharma, All India Institute of Medical Sciences, New Delhi - 110 049, India. E-mail: drpsharma57@yahoo.com

Received: 15-Oct-2020 Revision: 30-Jan-2021
Accepted: 20-Mar-2021 Published: 25-Aug-2021

Cite this article as: Panyala R, Sharma P, Sihota R, Saxena R, Prasad K, Phuljhele S, *et al*. Role of spectral domain optical coherence tomography in the diagnosis and prognosis of papilledema. Indian J Ophthalmol 2021;69:2372-7.

per A-scan. The HD 5 Line Raster scan, consisting of five speckles reduced B-scans of 9 mm long, each consisting of 1024 A-scans (each with an axial depth of 2 mm and 1024 pixels per A-scan) was performed. Using software provided with the SD-OCT the average retinal nerve fiber layer (RNFL) thickness for the total circumference was calculated.

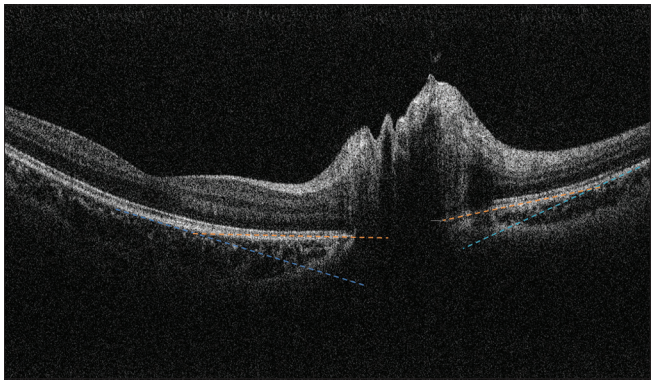

Figure 1: Spectral domain-optical coherence tomography (SD-OCT) 5 line raster scan image of papilledema patient showing positive angulation both on temporal and nasal sides. Blue line is the tangential line and orange line is along with the deviated retinal pigment epithelium/Bruch's membrane (RPE/BM)

Only good quality scans with a signal strength of at least six and centered on the optic disc, were included in the study. Temporal and nasal RPE/BM borders of the neural canal were identified on axial views evaluated from the individual B-scan (horizontal image) through the center of each optic disc. As described by Kupersmith *et al*.[2] in their study, the angle formed between the altered border adjacent to the NCO and a line drawn tangential to the curve of the unaltered RPE/BM in the peripapillary retina furthest from the ONH was measured on the nasal and temporal sides of the optic nerve [Fig. 1]. We evaluated the direction of the RPE/BM angle measured with the image centered on the optic disc and for all horizontal images above and below the midline. Because the angle direction was the same for all images at each NCO border in individual eyes, we analyzed the image positioned in the middle of the optic disc. The RPE/BM angle was considered positive when angulation was inward (towards the vitreous) and negative when the angulation was outward, on either the temporal or nasal border. A cut-off of 5° inward angulation (measured with Adobe Photoshop) was considered positive for this study. In all cases, we determined whether the angle was positive, negative, or neutral (called zero).

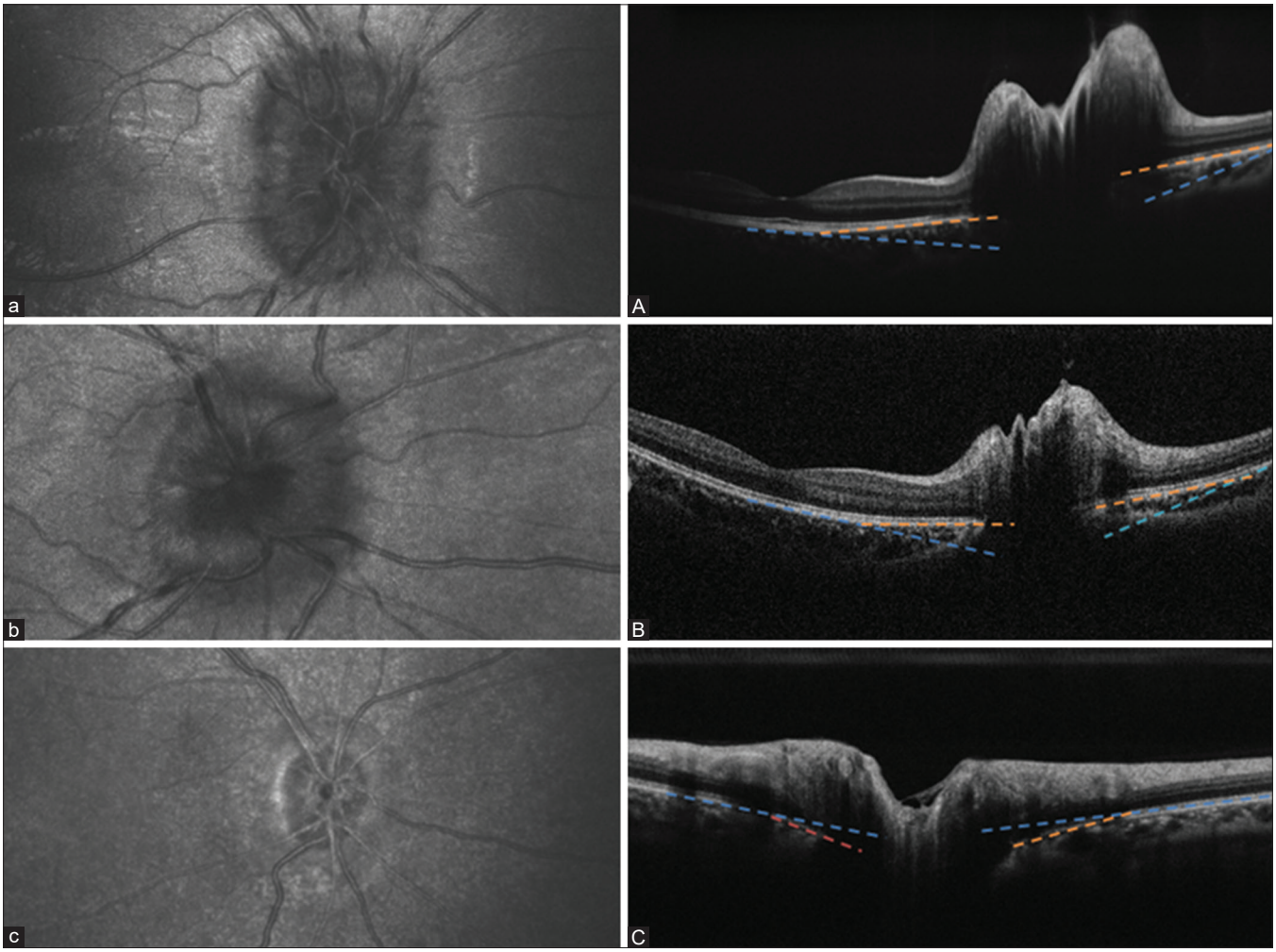

Figure 2: Optic disc images and SD-OCT 5 line raster scan image of Papilledema showing positive RPE/BM angle at baseline (a and A), at 1 month (b and B) and at 6 months (c and C) follow-up. Blue line is the tangential line and orange line is along with the deviated RPE/BM

Table 1: Comparison of Avg. RNFL thickness and RPE/BM angle among Papilledema, Papillitis and Controls

Parameters	Controls	Papilledema				Papillitis	
		Baseline	1 month	2 months	3 months	6 months	baseline	1 month
Avg. retinal nerve fiber layer thickness(μm)	95.5±28.19	167.29±67.03	121.15±68.47	113.87±37.56	103.63±29.79	97.34±29.74	141.64±55.52	115.17±37.60
P (vs controls)		<0.001	<0.01	0.03	0.077	0.08	<0.001	0.02
RPE/BM angle (T) (degrees)	−2.75±2.24	7.16±2.42	5.11±1.64	3.92±1.22	3.24±1.24	−1.24±1.02	−2.08±3.39	−2.25±2.25
P (vs controls)		<0.001	<0.001	0.01	0.019	0.13	0.089	0.09
RPE/BM angle (N) (degrees)	−1.22±3.12	8.11±3.13	5.21±1.85	4.32±1.31	3.56±1.76	−0.43±0.32	−1.04±3.27	−1.32±3.12
P (vs controls)		<0.001	<0.001	0.01	0.022	0.09	0.07	0.08

T=temporal, N=nasal. The above table illustrates the parameters namely average retinal nerve fiber layer thickness and RPE/BM angle (temporal and nasal side) in cases of papilledema, papillitis, and controls. The *P* value is calculated in comparison with controls and it was inferred that there was no significant difference in RPE/BM angle in papillitis patients and in cases of papilledema, average retinal nerve fiber layer thickness normalized at 3 months of follow-up whereas RPE/BM angle (nasal and temporal) was normalized at 6 months of follow-up. RPE/BM=retinal pigment epithelium/Bruch's membrane

Table 2: RPE/BM angle at 1-month follow-up in cases of papilledema and papillitis

Parameters	Papilledema	Papillitis	*P*
RPE/BM angle (T) (degrees)			
Baseline	7.16±2.42	−2.08±3.39	<0.001
1 month	5.11±1.64	−2.25±2.25	<0.001
RPE/BM angle (N) (degrees)			
Baseline	8.11±3.13	−1.04±3.27	<0.001
1 month	5.21±1.85	−1.32±3.12	<0.001

T=temporal, N=nasal. The above table illustrates the RPE/BM angle [temporal and nasal side] at 1-month follow-up in cases of papilledema and papillitis. There is a significant difference noted between the two groups both in the temporal and nasal baseline RPE/BM angle which persisted at 1-month follow-up

Table 3: Sensitivity and Specificity of RPE/BM angle in Papilledema

Temporal RPE/BM angle, taking cut-off as 5°			
Condition	Papilledema	Not papilledema	Total
Angle positive	29 (TP)	1 (FP)	30
Angle negative	1 (FN)	109 (TN)	110

Sensitivity = (true positive/diseased) × 100 = (29/30) × 100=96.66%.
Specificity = (true negative/not diseased) × 100 = (109/110) × 100=99.09%

Nasal RPE/BM angle, taking cut-off as 5°			
Condition	Papilledema	Not papilledema	Total
Angle positive	29 (TP)	1 (FP)	30
Angle negative	1 (FN)	109 (TN)	110

Sensitivity = (true positive/diseased) × 100 = (27/30) × 100=96.66%.
Specificity = (true negative/not diseased) × 100 = (85/95) × 100=99.09%. To detect papilledema, OCT measurement of RPE/BM angle has sensitivity of 96.66% and specificity of 99.09% on both nasal and temporal side

We evaluated the configurations of the optic nerve head and retinal layers around the optic nerve head and the average peripapillary RNFL thickness of the superior, inferior, nasal, and temporal quadrants in all patients. The RPE/BM angle (temporal and nasal), and average RNFL thickness for all four quadrants were calculated.

After baseline examination, patients with papilledema due to intracranial space-occupying lesions (ICSOLs) underwent surgical treatment of the lesions. Those diagnosed with idiopathic intracranial hypertension (IIH), cortical venous thrombosis, and meningitis were initiated or continued on medical therapy. Patients with papillitis were managed with intravenous methylprednisolone followed by oral prednisolone. All cases were followed up for 1 month. The papilledema patients were followed up further at 2, 3, and 6 months. Patients with IIH underwent lumbar puncture at baseline and at 6 months of follow-up. At all visits, anterior segment and posterior segment examinations were performed. There was no follow-up for controls.

Statistical analysis was performed using SPSS Ver. 20. The three groups were compared by Kruskal Wallis followed by Mann-Whitney test. Subgroup analysis was done by Wilcoxon sign ranked test.

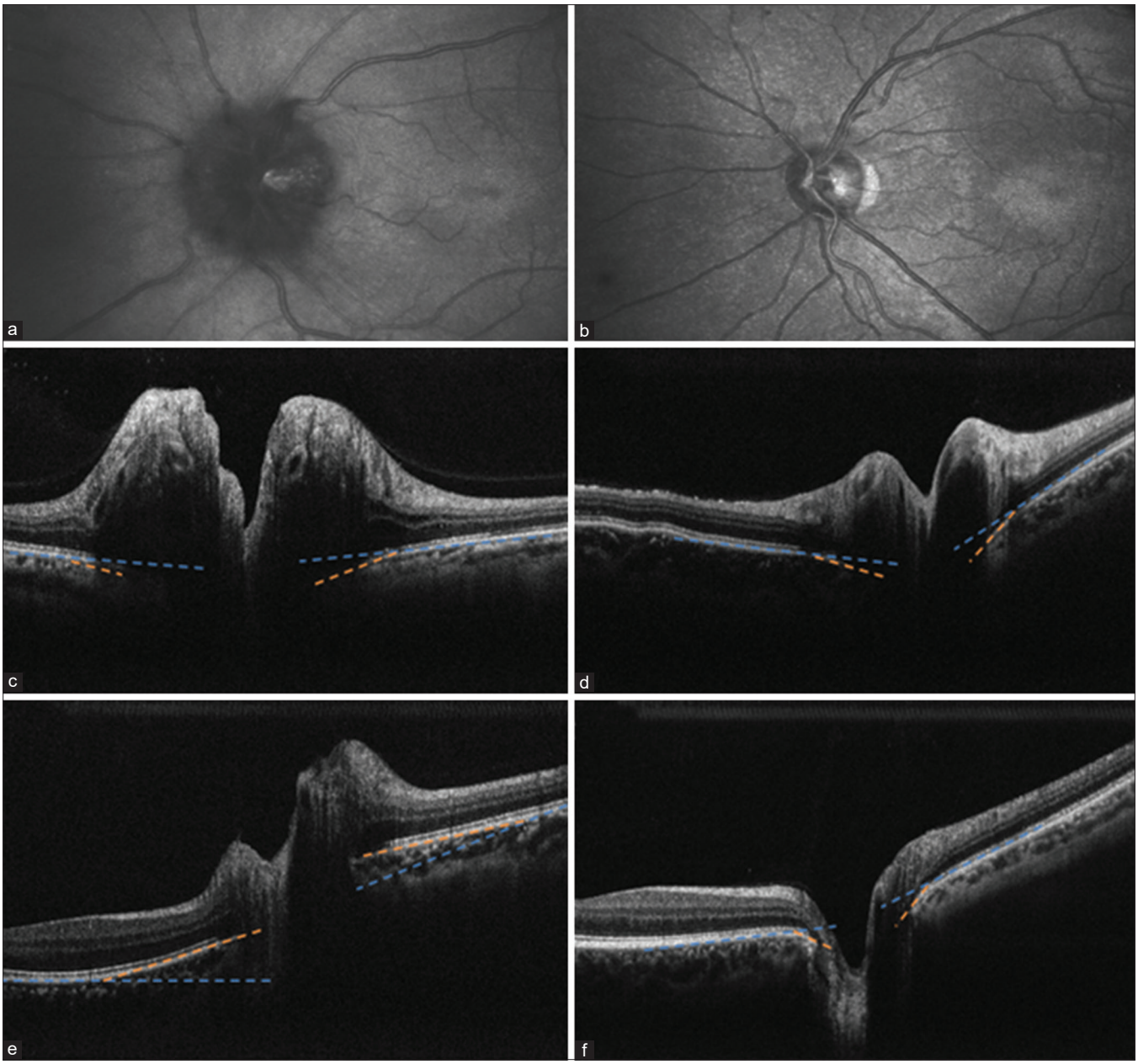

Figure 3: Optic disc image of papillitis at (a) baseline and at (b) 1-month follow-up. SD-OCT 5 line raster scan image of (c) Papillitis at baseline (d) papillitis patient at 1-month follow-up (e) Early Papilledema showing positive RPE/BM angle (f) OCT image in normal control. Blue line is the tangential line and orange line is along with the deviated RPE/BM

Results

A total of 60 eyes divided into two groups were recruited for the study—group 1 with 30 eyes of papilledema and group 2 with 30 eyes of papillitis associated with multiple sclerosis. Group 3 consisted of 80 eyes of controls. Mean age of group 1 was 25.6 ± 9.19 years, group 2 was 29.8 ± 7.29 and group 3 was 26.7 ± 4 years. All three groups were matched for age, sex, and laterality. Group 1 eyes were further divided into early or established papilledema based on clinical examination. The various etiologies of papilledema included IIH, meningitis, CVT, and ICSOL.

Comparison of eyes with papilledema and papillitis with control eyes is shown in Tables 1 and 2. At baseline, a significant difference was noted in baseline RNFL thickness between all three groups ($P < 0.001$). Of the 30 eyes with papilledema, 29 (96.6%) eyes had positive RPE/BM angle and 1 (3.3%) eye had negative angulation. Of the 30 eyes with papillitis, the RPE/BM angle was negative in 29 eyes (96.6%) and positive in 1 eye (3.3%). The nasal and temporal RPE/BM angles always corroborated with each other—none of the eyes showed positive angle on one side and negative angle on the other. There was a significant difference in baseline RPE/BM angle in papilledema when compared with papillitis [Table 1] (temporal angle $P = 0.01$; nasal angle $P = 0.01$) and controls [Table 1] (temporal angle $P = 0.01$; nasal angle $P = 0.01$) but no significant difference in baseline RPE/BM angle between the latter two ($P = 0.093$).

On follow-ups at 1, 2, 3, and 6 months, eyes with papilledema showed a reduction in the mean RNFL thickness with less positive RPE/BM angulation [Fig. 2]. However, subgroup analysis at 1 month of follow-up showed that early papilledema cases showed no significant difference in RNFL thickness (P = 0.07) when compared to controls, but a significant difference was seen in RPE/BM angle (P = 0.013). All eyes with papillitis had a significant reduction in RNFL thickness (P = 0.021) at 1 month but no significant difference in RPE/BM angle (temporal angle P = 0.203; nasal angle P = 0.086) [Fig. 3]. There was no significant difference in RNFL thickness between eyes with papilledema and papillitis at 1 month but significant difference persisted in RPE/BM angle (temporal angle P = 0.017; nasal angle P = 0.01) indicating a delayed resolution of angle deformation.

At 3 months, there was no significant difference in RNFL thickness (P = 0.07) compared to controls, but the difference in RPE/BM angle was significant (temporal angle P = 0.019; nasal angle P = 0.020) in eyes with papilledema.

At 6 months, neither RNFL thickness (P = 0.08) nor RPE/BM angle (temporal angle P = 0.13; nasal angle P = 0.09) showed significant difference compared to control eyes. On subgroup analysis, over 6 months of follow-up, 12 eyes with papilledema due to IIH had a significant decrease in RNFL thickness (P = 0.017) and RPE/BM angle (temporal angle P = 0.01; nasal angle P = 0.01), which was found to be proportional to the decrease in ICT. To detect papilledema, OCT has sensitivity of 96.66% and specificity of 99.09% on both nasal and temporal sides [Table 3].

Discussion

In papilledema, the increased ICT results in inward angulation of RPE/BM layer at NCO[3] unlike normal eyes and other causes of disc edema. Histopathology studies in animals have demonstrated that raised CSF pressure causes stasis of axoplasmic flow within the optic nerve sheath and decreases blood flow to the axons.[4-6] Subsequent vascular congestion, leakage, and ischemia are associated with interstitial edema. Because of its minimally invasive nature, ability for quick image acquisition, and high-resolution, cross-sectional image quality, OCT analysis of the optic disc has the potential to become an effective tool in the evaluation and management of patients with established or suspected papilledema and optic disc edema due to other causes.[1] Time-domain OCT is a useful technique for monitoring the severity of optic disc edema by measuring the thickness of the peripapillary RNFL.[7-9] SD-OCT measures the RNFL thickness and is a useful technique for assessing the structure of the optic disc in glaucoma and other optic neuropathies. It has also been used in the diagnosis and management of disc edema by quantifying a peripapillary RNFL thickness. Vartin *et al*.[10] used SD-OCT in reiterating the usefulness of total retinal thickness in increasing the sensitivity of detection of mild papilledema compared with conventional RNFL measurement. Johnson LN *et al*.[11] found that optic disc edema on OCT appeared as an elevated optic nerve head with smooth internal contour, with the sub-retinal hyporeflective space (SHYPS) at 1.5 mm radius being significantly thicker than twice that at the 2.0 mm radius. SD-OCT detects RNFL thickness[7,9,12,13] and various changes in subsurface architecture with much precision.[14] In spite of the fact that the sclera isn't imaged totally by SD-OCT, the angulation and displacement of the RPE/BM apparently indicate the deformation of the peripapillary sclera and lamina cribrosa occurring due to the increased pressure gradient between the globe and retrolaminar subarachnoid peri-optic nerve sheath compartment. However, all these studies were done on the western population. Our study emphasizes the role of SD-OCT in the diagnosis and monitoring of papilledema in Indian eyes.

Our findings are consistent with Morgan's experimental studies in dogs and Kupersmith *et al*.[2] on humans. Morgan,[15,16] using confocal scanning laser tomography, has shown that optic disc surface and lamina cribrosa displaces anteriorly on increased ICT and posteriorly on increased intraocular tension. Our study confirms the findings of Kupersmith *et al*.[2] that in cases of papilledema with intracranial hypertension, there is inward bowing of the RPE/BM layer at the NCO, not a finding in typical eyes or other forms of disc edema. This deformation is dynamic and opposite to that in glaucoma where outward RPE/BM angulation occurs but with a lower magnitude.[17] In chronic glaucoma, the increased IOP induces changes in the load-bearing structures leading to laminar thinning, posterior peripapillary scleral bowing, and expansion of the scleral canal.[15,16,18-22] As the normal lamina cribrosa is slightly bowed outward it is difficult to identify the posterior bowing in untreated glaucoma until a significant increase in the pressure gradient and damage to the structures of ONH occurs. Hence, inward bowing in raised ICT as in papilledema is easier to detect.

Papilledema patients might have differences in the deformation of the peripapillary RPE/BM owing to the subjective and regional variations in the compliance of the lamina cribrosa and peripapillary sclera. The study by Downs *et al*.[19,20] on peripapillary sclera in monkeys have shown that the nasal sclera is thin and more compliant to extraocular pressure than the temporal sclera. We found that with the increase in average RNFL thickness, there is a change in the RPE/BM angle with nasal being more than temporal, substantiating that in papilledema, the mean nasal RPE/BM angle was greater than the temporal. Also, when papilledema resolved, the nasal angle decreased faster than the temporal, probably owing to the increased compliance of the nasal sclera.

Our findings suggest that the degree of disc edema or RNFL thickening alone cannot explain the inward angulation of the peripapillary RPE/BM. The average RNFL thickness had no correlation with the degree of the positive angulation but in papilledema patients, the change in RNFL thickness altered the angulation of RPE/BM. In established papilledema, with increased thickening of the RNFL, there was an associated increase in positive angulation. In papillitis patients, with less negative RPE/BM angle (in the affected eye only), the angle became more negative as the RNFL thickening resolved, probably due to the extension of inflammation into the NCO altering the pressure gradient.

In our study, the RNFL thickness normalized at 3 months of follow-up and RPE/BM progressively decreased but normalized at 6 months of follow-up. In early papilledema cases, the RNFL thickness normalized at 1 month and RPE/BM angulation at 6 months of follow-up thus implying the role of RPE/BM angle as a better indicator of the disease activity than the RNFL thickness. One early papilledema patient (IIH) (3.3%) with ICP of 28 mmHg and normal intraocular pressure had a contradicting negative angulation of RPE/BM probably due to more negative premorbid RPE/BM angle. One patient with

papillitis (3.3%) had borderline positive angulation and it was normalized as the RNFL thickening resolved. This could have been due to the extension of inflammation into the NCO and alteration of the inward pressure gradient.

We also studied 12 eyes of papilledema due to IIH that had more positive baseline angulation compared to eyes with papilledema of other causes (*P* value 0.03). After initiation of treatment, the RPE/BM angle decreased in association with a decrease in RNFL thickness and at 6 months of follow-up, there was a significant decrease in ICP and improvement in visual functions with normalized RNFL thickness and RPE/BM angle. This finding is consistent with the study by Kupersmith *et al*.[2] and Wang *et al*.[21] where they described that the change in the peripapillary RPE/BM shape can be used as a potential biomarker to measure the success of treatment of raised ICP. We also studied early and established papilledema cases separately to find out whether the amount of RNFL thickness influences the RPE/BM angle and found that the established papilledema cases had more RNFL thickness and RPE/BM angulation than the early cases. In patients with early papilledema and papillitis having similar RNFL thickness and height of ONH swelling, the RPE/BM angulation was positive in early papilledema and negative in papillitis (which was similar to controls) thus rendering it as a useful diagnostic finding. We further studied and found that the sensitivity and specificity of RPE/BM to detect papilledema were 96.66% and 99.09% respectively, on both the nasal and the temporal side, which were higher compared to previous studies.

The deformative changes in the optic nerve may vary between two patients or each eye in the same patient as it depends on the degree of structural stiffness that again depends on the numerous anatomical factors.[18,22-24] The information on the premorbid RPE/BM angulation is important to preclude minor inward RPE/BM deformation. The limitations of our study include small sample size, constrained OCT penetration, treatment variation, and short follow-up. Although the reported angles were calculated and relative, this doesn't affect the direction of deviation.

Conclusion

Our study provides the SD-OCT evidence that increased ICP alters the peripapillary ONH and sub-surface structures and inward angulation of RPE/BM angle due to the pressure effect on the encompassing choroid, sclera, and lamina cribrosa. This study also shows that changes in the peripapillary RPE/BM occur over a short duration and owing to its delayed resolution, can be a useful parameter for the monitoring of papilledema. In conclusion, RPE/BM angle calculated through SD-OCT can be used to differentiate papilledema from papillitis and can also be used in monitoring disease activity in papilledema.

Financial support and sponsorship

Nil.

Conflicts of interest

There are no conflicts of interest.

References

1. Fujimoto JG, Brezinski ME, Tearney GJ, Boppart SA, Bouma B, Hee MR, *et al*. Optical biopsy and imaging using optical coherence tomography. Nat Med 1995;1:970-2.
2. Kupersmith MJ, Sibony P, Mandel G, Durbin M, Kardon RH. Optical coherence tomography of the swollen optic nerve head: Deformation of the peripapillary retinal pigment epithelium layer in papilledema. Invest Ophthalmol Vis Sci 2011;52:6558-64.
3. Gampa A, Vangipuram G, Shirazi Z, Moss HE. Quantitative association between peripapillary Bruch's membrane shape and intracranial pressure. Invest Ophthalmol Vis Sci 2017;58:2739-45.
4. Hayreh SS. Optic disc edema in raised intracranial pressure. V. Pathogenesis. Arch Ophthalmol 1977;95:1553-65.
5. Watson PG, Hayreh SS, Awdry PN. Episcleritis and scleritis. II. Br J Ophthalmol 1968;52:348-9.
6. Tso MO, Hayreh SS. Optic disc edema in raised intracranial pressure. IV. Axoplasmic transport in experimental papilledema. Arch Ophthalmol 1977;95:1458-62.
7. Scott CJ, Kardon RH, Lee AG, Frisén L, Wall M. Diagnosis and grading of papilledema in patients with raised intracranial pressure using optical coherence tomography vs clinical expert assessment using a clinical staging scale. Arch Ophthalmol 2010;128:705-11.
8. Knight RS, Fielder AR, Firth JL. Benign intracranial hypertension: Visual loss and optic nerve sheath fenestration. J Neurol Neurosurg Psychiatry 1986;49:243-50.
9. Rebolleda G, Muñoz-Negrete FJ. Follow-up of mild papilledema in idiopathic intracranial hypertension with optical coherence tomography. Invest Ophthalmol Vis Sci 2009;50:5197-200.
10. Vartin CV, Nguyen AM, Balmitgere T, Bernard M, Tilikete C, Vighetto A. Detection of mild papilloedema using spectral domain optical coherence tomography. Br J Ophthalmol 2012;96:375-9.
11. Johnson LN, Diehl ML, Hamm CW, Sommerville DN, Petroski GF. Differentiating optic disc edema from optic nerve head drusen on optical coherence tomography. Arch Ophthalmol 2009;127:45-9.
12. Menke MN, Feke GT, Trempe CL. OCT measurements in patients with optic disc edema. Invest Ophthalmol Vis Sci 2005;46:3807-11.
13. Rebolleda G, Diez-Alvarez L, Casado A, Sánchez-Sánchez C, de Dompablo E, González-López JJ, *et al*. OCT: New perspectives in neuro-ophthalmology. Saudi J Ophthalmol 2015;29:9-25.
14. Strouthidis NG, Grimm J, Williams GA, Cull GA, Wilson DJ, Burgoyne CF. A comparison of optic nerve head morphology viewed by spectral domain optical coherence tomography and by serial histology. Invest Ophthalmol Vis Sci 2010;51:1464-74.
15. Morgan WH, Chauhan BC, Yu D-Y, Cringle SJ, Alder VA, House PH. Optic disc movement with variations in intraocular and cerebrospinal fluid pressure. Invest Ophthalmol Vis Sci 2002;43:3236-42.
16. Morgan WH, Yu DY, Alder VA, Cringle SJ, Cooper RL, House PH, *et al*. The correlation between cerebrospinal fluid pressure and retrolaminar tissue pressure. Invest Ophthalmol Vis Sci 1998;39:1419-28.
17. Fortune B, Yang H, Strouthidis NG, Cull GA, Grimm JL, Downs JC, *et al*. The effect of acute intraocular pressure elevation on peripapillary retinal thickness, retinal nerve fiber layer thickness, and retardance. Invest Ophthalmol Vis Sci 2009;50:4719-26.
18. Burgoyne CF, Downs JC, Bellezza AJ, Suh J-KF, Hart RT. The optic nerve head as a biomechanical structure: A new paradigm for understanding the role of IOP-related stress and strain in the pathophysiology of glaucomatous optic nerve head damage. Prog Retin Eye Res 2005;24:39-73.
19. Downs JC, Blidner RA, Bellezza AJ, Thompson HW, Hart RT, Burgoyne CF. Peripapillary scleral thickness in perfusion-fixed normal monkey eyes. Invest Ophthalmol Vis Sci 2002;43:2229-35.
20. Downs JC, Ensor ME, Bellezza AJ, Thompson HW, Hart RT, Burgoyne CF. Posterior scleral thickness in perfusion-fixed normal and early-glaucoma monkey eyes. Invest Ophthalmol Vis Sci 2001;42:3202-8.
21. Wang J-K, Kardon RH, Ledolter J, Sibony PA, Kupersmith MJ, Garvin MK. Peripapillary retinal pigment epithelium layer shape changes from acetazolamide treatment in the idiopathic intracranial hypertension treatment trial. Invest Ophthalmol Vis Sci 2017;58:2554.
22. Sigal IA, Flanagan JG, Tertinegg I, Ethier CR. 3D morphometry of the human optic nerve head. Exp Eye Res 2010;90:70-80.
23. Killer HE, Laeng HR, Flammer J, Groscurth P. Architecture of arachnoid trabeculae, pillars, and septa in the subarachnoid space of the human optic nerve: Anatomy and clinical considerations. Br J Ophthalmol 2003;87:777-81.
24. Sigal IA, Flanagan JG, Ethier CR. Factors influencing optic nerve head biomechanics. Invest Ophthalmol Vis Sci 2005;46:4189-99.